Isotope Effects and the Mechanism of Atom Transfer Radical Polymerization

Daniel A. Singleton,*,† Daniel T. Nowlan III,† Nazeem Jahed,‡ and Krzysztof Matyjaszewski*,‡

Department of Chemistry, Texas A&M University, PO Box 30012, College Station, Texas 77842, and Department of Chemistry, Carnegie Mellon University, 4400 Fifth Avenue, Pittsburgh, Pennsylvania 15213

Received September 4, 2003

ABSTRACT: The mechanism of free-radical polymerization and atom transfer radical polymerization (ATRP) of methyl methacrylate was studied by a combination of ^{13}C kinetic isotope effects and theoretical calculations. Free-radical polymerization initiated by AIBN and ATRP initiated by 1:2:1 CuBr:2,2′-bipyridine:ethyl 2-bromoisobutyrate exhibit statistically indistinguishable ^{13}C isotope effects. This supports identical chain-propagation steps in ATRP and free-radical polymerization. The free-radical additions leading to these isotope effects were modeled in DFT calculations of transition structures for the addition of 2-methoxycarbonyl-2-propyl radical to methyl methacrylate. Comparison of predicted isotope effects with the experimental values supports the approximate accuracy of the DFT transition structures vs the physical transition state but suggests that the predicted transition structures are slightly too early. This suggestion is supported by comparison of DFT predictions with high-level ab initio predictions in the simpler addition of methyl radical to ethylene. In light of the evidence here and in the literature supporting a free-radical addition at the core of the ATRP mechanism, the often-proposed intervention of metal−radical complexes in either ATRP or the mechanistically parallel atom transfer radical addition reactions is critically evaluated.

In controlled/living radical polymerization (CRP), the equivalent of a traditional free-radical polymerization is carried out under conditions designed to maintain a low, stationary concentration of an active reactant in dynamic equilibrium with dormant but ultimately extensible polymer chains.[1−3] Because of its experimental simplicity and utility in accessing well-defined (co)polymers, CRP has attracted exceptional interest and may lead to many potential commercial applications. One particularly robust form of CRP is atom transfer radical polymerization (ATRP).[4−9] In ATRP, the polymerization is mediated by a combination of a transition-metal complex and an initiating alkyl halide, with the halide attached to the ends of the polymer chains in their dormant form. ATRP is particularly robust because it involves undemanding reaction conditions and is effective with a variety of polymerizable monomers and functional (macro)initiators.

ATRP is an extension of the atom transfer radical addition (ATRA) reactions of Kharasch.[10] In ATRA, the 1:1 addition of an alkyl halide to an alkene is catalyzed by either free-radical initiators or transition-metal complexes. When catalyzed by free-radical initiators, the mechanism is a simple free-radical chain process (Scheme 1). Transition-metal catalysts can mediate a similar mechanism (Scheme 2) by forming radicals in a redox process (eq 4) and promoting "chain transfer" by donating a halide to the adduct radical (eq 6).[11] However, there are often large differences in the outcome of free-radical-initiated vs transition-metal-catalyzed ATRA reactions, the latter particularly minimizing telomerization. For this reason, alternative reaction mechanisms that invoke metal-complexed radicals have been suggested.[12−18] Mechanistic studies have at times weighed against alternative mechanisms,[19,20] and direct evidence for often-postulated loose metal−radical complexes has been notably lacking. The role of the metal catalyst in effecting the final product formation/chain transfer of eq 6 would appear to account for many of the differences between the free-radical-initiated and metal-catalyzed reactions. However, the exceptional diversity of reactions, catalysts, and observations fetters any sweeping mechanistic analysis of ATRA reactions.

Scheme 1. Mechanism of Free-Radical-Initiated ATRA

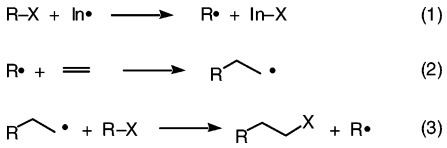

Scheme 2. Redox Mechanism for Metal-Catalyzed ATRA

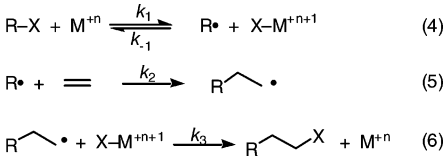

ATRP was designed to be mechanistically analogous to the transition-metal-catalyzed ATRA. In the proposed mechanism, the metal catalyst promotes reversible generation of free radicals from the halide-terminated polymer chains. The chain-extension step would then be a simple free-radical addition to monomer with no metal involvement.

† Texas A&M University.
‡ Carnegie Mellon University.
* Corresponding authors: e-mail singleton@mail.chem.tamu.edu; km3b@andrew.cmu.edu.

10.1021/ma035310r CCC: $25.00
Published on Web 10/25/2003

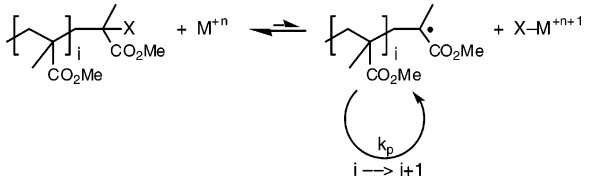

A large number of observations are consistent with this mechanism for ATRP. Monomer reactivity ratios are similar to those reported for conventional free-radical polymerizations,[21−23] although some effect of solvent, dilution, and intermittent activation on these ratios is expected.[1,23,24] The polymerizations are quenched efficiently with radical traps such as galvinoxyl and TEMPO.[25] There is a negligible effect of protic impurities such as water and alcohols.[26,27] The equilibrium of eq 4 can be approached from the other side, using Cu(II)/AIBN as the initiating system.[28,29] Under ATRP/ATRA conditions, methyl 2-bromopropiontate undergoes racemization, halogen exchange, and trapping with TEMPO at identical rates, supporting the forward step of eq 4 as rate limiting.[30] Using Cu(I) catalysts, the evolution of Cu(II) measured by EPR conforms to expectations for the persistent radical effect.[31,32] EPR has also directly detected growing radicals in the polymerization of dimethacrylates.[33] Identical rate constants were found for additions to alkenes in Cu/bpy-catalyzed ATRA vs additions of radicals generated via flash photolysis.[34]

In contrast, a number of observations have been interpreted as suggesting a much more complex role for the metal catalyst in the ATRP mechanism. Haddleton found that even large amounts of phenols do not inhibit ATRP of methyl methacrylate.[35] Expecting such inhibition for a free-radical process, Haddleton concluded that a "normal" free-radical mechanism was not operative. Changes in the reaction medium, such as using aqueous or oxyethylene solvents, can substantially affect the rate.[36,37] Very recently, Harrison, Rourke, and Haddleton (HRH) have measured ^{13}C kinetic isotope effects (KIEs) for polymerizations of methyl methacrylate.[38] In their competition reactions at natural abundance, the observed isotope effects should reflect the transition state for incorporation of methacrylate monomer into the growing chain. Most interestingly, HRH observed different isotope effects for ATRP (using *N*-propyl-2-pyridinylmethanimine/CuBr catalyst) vs classical free-radical polymerizations (Figure 1). If correct, their observations would be strong evidence that at least some of the ATRP chain growth was occurring by a process other than a simple free-radical addition.

The mechanism of ATRP and ATRA reactions is intriguing from a fundamental perspective, but it also has a critical practical impact on the further development of these reactions. If a metal complex is involved in the addition step, then it should be malleable for use in diverse ways as a reaction control element. If variations in catalyst structure can only impact the rates of the forward and reverse reactions of eq 4, then the impact of catalyst modifications will be much more limited.

We describe here a combined experimental and theoretical study of the mechanisms of ATRP and free-radical-mediated polymerizations of methyl methacrylate. Using a comparison of observed and predicted KIEs for the radical polymerization, along with high-level calculations on simple radical additions, we are able to gauge the accuracy of DFT calculations in their description of the transition-state geometry for these reactions. In this way, the observed KIEs are used to delineate an experimentally based transition-state geometry for the free-radical additions that effect the polymerization. The isotope effects observed here for ATRP (MMA catalyzed by CuBr/2,2′-bipyridine) are identical to those for free-radical polymerization, weighing strongly against involvement of the metal catalyst in the addition steps of ATRP. In light of these findings, we suggest a reinterpretation of a variety of literature observations.

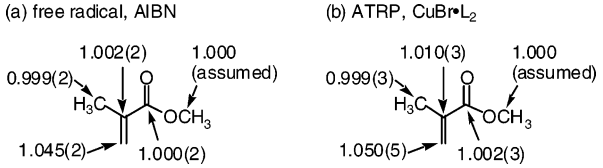

Figure 1. ^{13}C KIEs (k^{12}_C/k^{13}_C, 60 °C) from ref 38 for polymerizations of methyl methacrylate in xylenes. (a) Free-radical polymerization initiated by AIBN. (b) ATRP initiated by 1:2:1 CuBr:*N*-propyl-2-pyridinylmethanimine:ethyl 2-bromoisobutyrate.

Results

Experimental Isotope Effects. The free-radical polymerization of ≈5 M methyl methacrylate in 1,2-dichlorobenzene catalyzed by 0.3 mol % AIBN was studied at 80 °C. Under these conditions, reactions taken to 50%−90% conversion afforded polymers with molecular weights of 40 000−50 000 and polydispersities of ≈1.8. The ^{13}C KIEs for this reaction were measured at natural abundance by NMR methodology.[39] Quadruplicate reactions taken to 80−95% conversion were quenched by the addition of hydroxy-TEMPO after cooling and opening to air, and the unreacted methyl methacrylate was recovered by three successive fractional vacuum distillations. The samples of recovered methyl methacrylate were analyzed by ^{13}C NMR along with standard samples of the original methyl methacrylate not subjected to the reaction conditions. The changes in isotopic conversion were determined relative to the methyl ester carbon, assuming that its isotopic composition does not change. From the changes in isotopic composition, the ^{13}C isotope effects were calculated as previously described.[39]

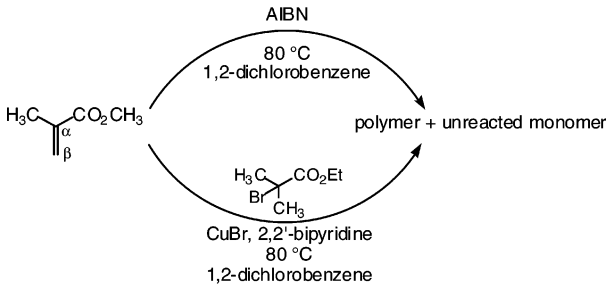

The KIEs for the ATRP polymerization of methyl methacrylate were studied in an analogous fashion. Polymerizations of methyl methacrylate initiated with 0.5% CuBr, 1% 2,2-bipyridine, and 0.5% ethyl 2-bromoisobutyrate at 80 °C were taken to ≈80% conversion, affording polymers with molecular weights of ≈17 000 and polydispersities of ≈1.29. The unreacted methyl methacrylate from quenched reactions was then analyzed by ^{13}C NMR as described above.

Table 1. Experimental and Theoretical ^{13}C KIEs ($k_{^{12}C}/k_{^{13}C}$, 80 °C) for Free-Radical Additions and ATRP

	Cβ	Cα	C(=O)	α-CH_3
		Experimental KIEs[a]		
free radical[b]				
exp 1	1.040(2)	1.007(1)	1.002(1)	1.000(1)
exp 2	1.041(2)	1.007(2)	1.002(1)	1.002(2)
exp 3	1.043(5)	1.009(4)	1.002(4)	1.000(3)
exp 4	1.039(4)	1.007(3)	1.004(3)	0.998(3)
ATRP[c]				
exp 1	1.043(5)	1.006(3)	1.003(3)	1.001(4)
exp 2	1.046(5)	1.007(3)	1.000(3)	1.001(3)
exp 3	1.040(2)	1.007(1)	1.003(2)	1.001(2)
exp 4	1.041(2)	1.006(2)	1.003(1)	1.001(1)
		Theoretical KIEs		
ethylene + $•CH_3$				
UCCSD(T)/6-311+G**	1.038	1.006		
UCCSD(T)/6-31G*	1.040	1.007		
UQCISD/6-31G*	1.042	1.008		
UB3LYP/6-311+G**	1.034	1.008		
UB3LYP/6-31G*	1.032	1.007		
UMPW1K/6-31+G**	1.034	1.008		
acrolein + **7**[d]				
UQCISD/6-31G*	1.040	1.006	0.999	
UB3LYP/6-311+G**	1.034	1.006	1.002	
UB3LYP/6-31G*	1.033	1.005	1.002	
UMPW1K/6-31+G**	1.035	1.007	1.003	
methyl methacrylate + **1**[e]				
UB3LYP/6-311+G**	1.0388	1.0070	1.0022	1.0009
UB3LYP/6-31G*	1.0378	1.0071	1.0023	1.0009
UMPW1K/6-31+G**	1.0387	1.0076	1.0018	1.0008

[a] Because the KIE determination assumes that the isotope composition of the methyl ester carbon does not change, the experimental KIEs are "relative" to the methyl ester KIE. The predicted KIE for the methyl ester carbon of methyl methacrylate was in each case 1.000. [b] Free-radical polymerization initiated by AIBN. [c] ATRP initiated by 1:2:1 CuBr:2,2′-bipyridine:ethyl 2-bromoisobutyrate. [d] Predicted for the transition structure conformer in Figure 2b. See ref 44. [e] Predicted for the transition-state conformer **10**. Among other UB3LYP/6-31G* transition structures for the addition of **1** to methyl methacrylate, the predicted KIEs varied from those for **10** by less than 0.001.

For both the free-radical polymerizations and the ATRP, the KIEs were determined for four independent reactions, with six NMR KIE measurements on each reaction. The results are summarized in Table 1. As might be expected qualitatively, all of the reactions exhibit a large KIE at Cβ and small isotope effects at the carbonyl carbon and vinylic methyl group. Interestingly, all of the reactions exhibit a significant Cα KIE. This isotope effect, as well as the similarity of the free-radical and ATRP KIEs, will be analyzed in more detail below.

Theoretical Calculations. The addition of 2-methoxycarbonyl-2-propyl radical (**1**) to methyl methacrylate was chosen as the theoretical model for the free-radical polymerization of methyl methacrylate. For the purpose at hand of interpreting the experimental KIEs, the ideal calculation in one that leads to accurate KIE predictions for the mechanism calculated. In general, this requires both accurate transition-state geometries and accurate frequencies (both real and imaginary) at the transition state. The size of the reaction here precludes the use of very high level ab initio methods. UHF calculations afford reasonable geometries for radical addition reactions,[40] but HF calculations have not been entirely adequate for the prediction of KIEs.[41] This leaves us with DFT methods, and hybrid DFT calculations (UB3LYP or UMPW1K) were applied to the addition of **1** (Scheme 3) to methyl methacrylate. However, there was some reason to be concerned over the adequacy of the DFT methods for this reaction. Early observations suggested that UBLYP transition-state geometries for alkyl radical additions were too early.[40] Some literature studies have supported the applicability of UB3LYP calculations in simple radical addition reactions,[42] but

Scheme 3

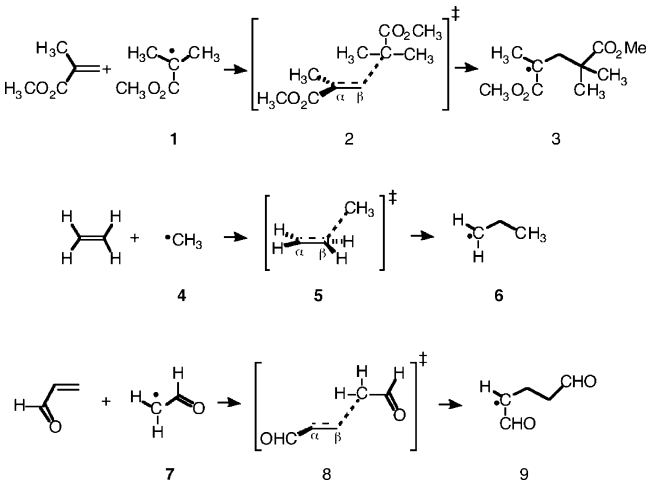

the UB3LYP/6-31G* transition state for addition of methyl radical to ethylene is notably earlier than that predicted by UQCISD(T)/6-31G* calculations.[40] UB3LYP calculations do not fare well in predicting the overall energetics for this addition, particularly with large basis sets.[43]

To better delimit the accuracy of the UB3LYP and UMPW1K calculations in smaller systems, transition structures for the addition of methyl radical (**4**) to ethylene and the addition of formylmethyl radical (**7**) to acrolein[44] were fully optimized at a series of calculational levels. The results are summarized in Figure 2. The highest level ab initio calculations applied to these reactions appear to afford reasonable predictions of geometries and energies in other radical reactions,

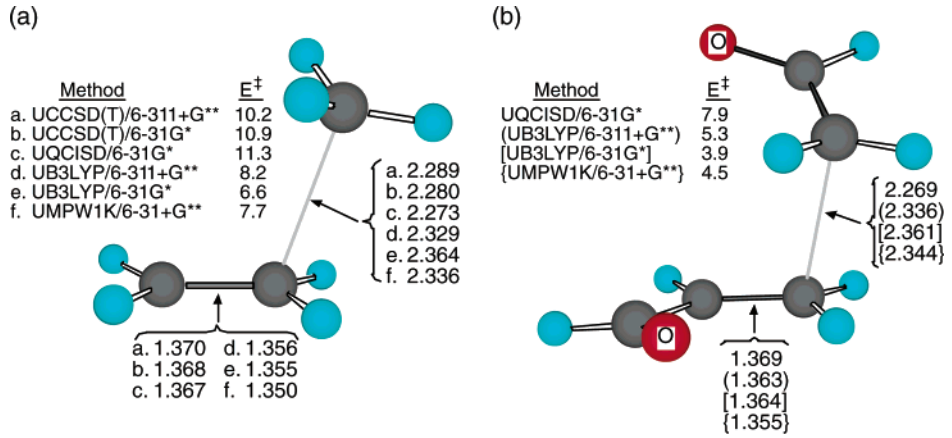

Figure 2. Transition structures for (a) the addition of methyl radical to ethylene and (b) the addition of formylmethyl radical to acrolein. Calculated reaction barriers (including zpe) are given in kcal/mol, and distances are given in angstroms.

despite some concern over spin contamination.[45] For both reactions the DFT methods predict lower addition barriers than the best ab initio structures by 2−4 kcal/mol. The experimental activation energy for the addition of **4** to ethylene is 7.9 kcal/mol,[46] and the DFT calculations are more accurate in predicting this barrier. It should be noted that the phenomenological activation barrier determined from Arrhenius plots may differ significantly from the true barrier.[47] However, the inference that even the UCCSD(T)/6-311+G** calculation is overestimating the reaction barriers is also supported by a single-point calculation using a very large basis set (UCCSD(T)/aug-cc-pVTZ//UCCSD(T)/6-31/6-311+G** + zpe), which lowers the predicted barrier to 8.7 kcal/mol. As found in previous work, the UB3LYP transition structures for the addition of **4** to ethylene are earlier than the ab initio structures. The use of increasingly large basis sets seems to bring the UCCSD(T) and UB3LYP structures toward each other, though for the UB3LYP calculation the later transition state obtained with a bigger basis set seems connected to a general skewing of the reaction coordinate—the UB3LYP/6-311+G** calculation underestimates the enthalpy of reaction by ≈3 kcal/mol. With such an error in the reaction enthalpy, the excellent prediction of the barrier at the UB3LYP/6-311+G** level appears to be in part fortuitous.

The addition of **7** to acrolein was studied because the conjugation in the reactants closely resembles the **1**/methyl methacrylate reaction of interest, yet the system is small enough to allow a UQCISD calculation. The results with **7**/acrolein closely mirror the trends in activation barrier and transition structure bond lengths seen in the addition of **4** to ethylene. From this similarity, we infer that the ab initio trends observed in the addition of **4** to ethylene would also be observed for the addition of **1** to methyl methacrylate, were such calculations feasible. In both the addition of **4** to ethylene and **7** to acrolein, the difference between DFT and ab initio structures is small—a few hundredths of an angstrom in the forming C−C bond—but it will be seen that the geometry difference is reflected in predicted KIEs. Conversely, the observed KIEs will allow us to gauge the accuracy (or systematic inaccuracy) of the DFT calculations in the experimental system.

The addition of **1** to methyl methacrylate is complicated by a multitude of possible transition structures. A total of 12 transition structures were located in UB3LYP/6-31G* calculations, arising from six diastereomeric orientations of **1** in additions to either s-cis or s-trans conformers of methyl methacrylate. All 12 structures are similar in energy, within a range of 1.5 kcal/mol. The lowest energy structure (including zpe and an entropy estimate at 25 °C based on the harmonic frequencies) was **10**; all 12 are shown in the Supporting Information. There was a small general preference for addition to the s-cis conformer of methyl methacrylate—the best addition to the s-trans conformer was 0.5 kcal/mol higher in energy. Structure **10** was reoptimized in UB3LYP/6-311+G** and UMPW1K/6-31+G** calculations, but there is very little difference between these structures. The predicted barriers of ≈6−9 kcal/mol for the addition reaction via **10** are in reasonable agreement with the experimental activation barrier of 5.5 ± 1.1 kcal/mol.[48]

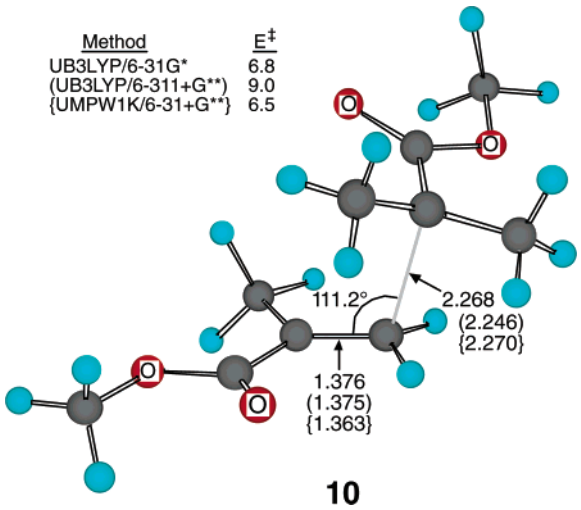

10

Predicted Isotope Effects. For each of the calculated transition structures, ^{13}C KIEs were predicted from the scaled theoretical vibrational frequencies[49] by the method of Bigeleisen and Mayer.[50] Tunneling corrections were applied using the one-dimensional infinite parabolic barrier model.[51] Previous work has supported the necessity of such tunneling corrections and the adequacy of one-dimensional corrections for reactions having normal barriers and not involving hydrogen transfer.[41b] Overall, ^{13}C KIE predictions based on DFT and post-HF calculations have proven highly accurate in neutral reactions not involving hydrogen transfer, so long as the calculation accurately depicts the mechanism and transition-state geometry.[41,52]

The results are summarized in Table 1. All of the calculations predict a large ^{13}C KIE at the olefinic carbon undergoing addition (referred to as Cβ in each case) and a significant ^{13}C KIE of 1.005−1.008 at the distal olefinic carbon (Cα). The Cα KIE appears associated with weakening of the bonding to Cα. For example, the two vibrational modes associated with Cβ═Cα stretching decrease from 1720 and 1395 cm^{-1} in ethylene (B3LYP/6-31G*, unscaled frequencies) to 1616 and 1326 cm^{-1} in the UB3LYP/6-31G* transition structure. The Cα KIEs in radical additions may be contrasted with the much smaller ^{13}C KIEs at C2 and C3 of isoprene (1.001−1.002) in its Diels−Alder reaction with maleic anhydride.[41a] In the Diels−Alder reaction, the simultaneous formation of a full new π bond compensates for the breaking of the original π bonds, while in radical additions the total bonding to Cα is decreasing.

For the addition of **4** to ethylene, the magnitude of the Cβ KIE varies inversely with the length of the forming Cβ- -CH_3 bond. If the UCCSD(T)/6-311+G** structure is assumed, for now, to be the most accurate and is taken as a standard, then the UCCSD(T)/6-31G* and UQCISD/6-31G* structures lead to KIE predictions that are slightly too high (by 0.002 and 0.004, respectively). The earlier DFT transition structures consistently lead to lower predicted KIEs (0.004 lower for the UB3LYP/6-311+G** and UMPW1K/6-31+G** structures). The change to a conjugated radical and acceptor in the addition of **7** to acrolein does not affect the basic trend—the Cβ KIE predicted for the transition structures from DFT methods is 0.007−0.005 lower than the KIE for the later UQCISD transition structure. This observation suggests that, if they were possible, high-level ab initio calculations on the addition of **1** to methyl methacrylate would also result in slightly later transition structures and higher KIEs than the DFT structures.

Discussion

Our plan in this discussion is to first use the combination of experimental isotope effects and theoretical calculations to delimit the transition state for the addition of **1** to methyl methacrylate and to comment on the geometrical accuracy of calculated transition states for radical additions. We then analyze the KIEs for ATRP and address the mechanism of ATRP. Finally, we present some comments and cautions on the interpretation of experimental observations in considering the mechanism of ATRP and ATRA reactions in general.

To define the physical transition-state geometry for the addition of **1** to methyl methacrylate, we first consider the accuracy of the computational methods applied. For the much simpler reaction of methyl radical with ethylene, it is possible to compare the DFT predictions with very high-level ab initio calculations. It might normally be assumed that the UCCSD(T) predictions employing a large basis set are highly accurate. Such calculations perform well in other simple radical reactions; for example, the predicted classical barrier for hydrogen abstraction from methane by hydroxyl radical at the UCCSD(T)/6-311+G** level is 6.7 kcal/mol, compared to an estimate based on experimental rate constants and dynamics calculations of 7 kcal/mol.[45] However, with basis sets amendable to geometry optimization, the ab initio barriers for the addition of methyl radical to ethylene are too high. For a highly exothermic reaction involving a low barrier, error raising the barrier could potentially make the saddle point too late. (This trend is exhibited well in the series of structures in Figure 2a.) This does not mean that the DFT transition structures are more accurate than the ab initio structures, only that it cannot be simply assumed at this point that the ab initio structures are geometrically more accurate.

Comparison of the experimental and predicted KIEs is helpful in addressing this issue. If the eight sets of KIEs from free-radical and ATRP reactions are statistically combined (see the justification below), the composite values are 1.0416 ± 0.0018, 1.0070 ± 0.0007, 1.0024 ± 0.0010, and 1.0005 ± 0.0010 (uncertainties are 95% confidence) for the Cβ, Cα, carbonyl, and α-CH_3 carbons, respectively. The predicted KIEs in Table 1 match the experimental values phenomenally well at three of the four positions—except for Cβ, all of the predictions are well within experimental error. For Cβ, the predicted KIEs are too low, but only by 0.003−0.004. This is close to the difference between the predicted KIEs for the UB3LYP/6-311+G** or UMPW1K/6-31+G** levels vs UCCSD(T)/6-311+G**. The most important conclusion from this close correlation of experimental and predicted KIEs is that the calculated DFT transition structures are an approximately accurate depiction of the physical transition state. However, interpreting the data to its limits, the too-low prediction of Cβ supports the idea that the DFT structures for the addition of **1** to methyl methacrylate are slightly too early. If this idea is applied to the addition of methyl radical to ethylene, then the UCCSD(T)/6-311+G** structure must be very close to reality.

The experimental isotope effects shown in Table 1 for free-radical polymerization vs ATRP are obviously very similar. All 32 of the measured KIEs are within their standard deviation of the average Cβ, Cα, carbonyl, and α-CH_3 KIEs above. The average of the Cβ results for ATRP is greater than the average of Cβ results for free-radical polymerization (1.0425 vs 1.040 75, a difference of 0.001 75), and it might be wondered whether this signifies some difference between the sets of results. To test this statistically, we set up a spreadsheet in which eight results randomly varied from a "true" value of 1.0416 in a Gaussian distribution using the experimental standard deviations. Average KIEs from sequential sets of four results differed by 0.001 75 or greater 46% of the time. From this, we conclude that the observed difference between free-radical and ATRP results is in accord with a typical random-chance effect. The ATRP and free-radical polymerization results are thus statistically indistinguishable. Although it can never be ruled out that some unknown alternative mechanism exhibits KIEs equivalent to the free-radical KIEs, the results here are best interpreted as strongly supporting identical chain-propagation steps in ATRP and free-radical polymerization.

What about the HRH results in Figure 1?[38] Considering the difference in temperature and the experimental uncertainties, almost all of their observed KIEs are consistent with those observed here. Only one does not fit—the Cα result of 1.002 in the free-radical polymerization. All of the theoretical calculations predict a much larger Cα KIE than 1.002, for reasons described above, and it is not clear how a free-radical process could exhibit such a small Cα effect. The result would appear to be anomalous.[53] For ATRP, the HRH Cα KIE of 1.010

± 0.003 at 60 °C is notably consistent with theoretical predictions for a free-radical process.

The observations here, along with diverse observations described in the Introduction, weigh against an important role for metal−radical complexes in ATRP. By implication, these results speak to ATRA reactions as well. We consider here in general terms the observations that weigh oppositely, that is, have been taken to support a role for metal−radical complexes in ATRP or ATRA reactions. The simplest of these is the differing reaction outcomes vs simple free-radical-initiated reactions. Free-radical polymerization and ATRP exhibit importantly (and usefully) different characteristics; the same is true for free-radical-initiated vs transition-metal-catalyzed ATRA reactions. It is necessary to explain, at least in overview, how such different traits can arise without involvement of metal−alkene or metal−radical complexes. In any reaction, kinetic product mixtures are the result of competitive pathways. The attribution of changes in product composition to a mechanistic change in the major pathway is perhaps intuitively attractive, but it is equally possible for the outcome of a reaction to change due to changes in side processes. Owing to the persistent radical effect,[32,54] side reactions from free-radical chain processes are controlled by the rapidly formed abundance of the most persistent radical. In free-radical polymerization, the most persistent radicals are carbon radicals that undergo recombination or disproportionation, terminating polymer chains. In free-radical-initiated ATRA, the abundant carbon radicals may undergo undesired telomerization rather than a desired chain transfer. In contrast, in ATRP or transition-metal-catalyzed ATRA reactions, the persistent "radical" is an oxidized metal halide. ATRA may be viewed as taking advantage of the "side reaction" of the abundant metal halide with carbon radicals to afford the desired addition product. Since the metal halide complex is present in the product-forming step, it should not be surprising that the complex can influence some aspects of product stereoselectivity.[12,17] In ATRP, reaction of the oligomeric carbon radicals with the metal halide occurs reversibly to afford the dormant chain. Overall, by changing the persistent radical, the qualitative characteristics of reactions can change dramatically. The mechanistic ideas in this paragraph are not new,[30−34,55] but their consideration should serve to emphasize the tenuity of previous arguments for metal mediation of additions based on product observations.[12,13,15,17,18]

Kinetic studies have been used to support a role for metal−radical complexes in ATRA reactions. The key observation in such studies has been a rate law that is first-order in the transition-metal catalyst.[15,18,56,57] If the metal complex were simply acting as an initiator in ATRA reactions, the rate law would be half order in complex, as is typical for free-radical initiators. However, from the persistent radical effect, the concentration of the oxidized metal halide ($X-M^{+n+1}$) in these reactions will tend to increase with time, so kinetic observations are likely to be complex. To briefly study this issue, we simulated the kinetics for an ATRA reaction following the mechanism of Scheme 2 by numerically integrating the kinetic equations. (See Supporting Information for the computational program.) In this simulation, the apparent rate law that would be observed from a study of initial rates varies substantially depending on the assumed rate constants, but it was readily possible to identify sets of rate constants that would engender ostensible unimolecularity in the catalyst. For example, if k_1, k_{-1}, k_2, and k_3 in Scheme 2 were 1, 10^6, 10^4, and 10^6 M^{-1} s^{-1}, respectively, the kinetics would appear to be approximately first order in both M^{+n} and the alkene.[58] This suggests that great caution should be used in interpreting kinetic studies of these reactions.

As an alternative to free radicals in ATRP or ATRA reactions, "caged" radical complexes or "radicals within the coordination sphere" (e.g., **11** or **12**) have routinely been postulated.[12,15,17,18,38] It seems worthwhile to point out that such species do not seem physically reasonable as intermediates with sufficient lifetimes for reactivity. Unbound radical pairs should separate at essentially a diffusion-controlled rate. Alternative intermediates in which the carbon radicals are discretely bound to the metal have not been considered viable, in part because of the resulting disfavored oxidation states (e.g., Ni(IV) or Ru(IV)) and in part because of the characteristically radical-like reactivity observed in these reactions.

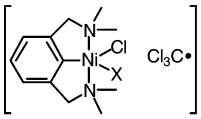

11

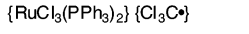

12

For ATRP, the observation that phenols are not inhibitors may seem striking at first glance.[35] However, it had long ago been found that phenols afford negligible chain transfer and inhibition in free-radical-initiated polymerizations of methacrylates, *in the absence of oxygen*.[59] Oxygen has long been known to play a critical supporting role in the action of many free-radical inhibitors;[60] in its absence, a low rate for hydrogen transfer from phenols to the relatively stable radicals derived from methacrylates should not be surprising. The observation in cases of substantial effects of the reaction medium on the rate of ATRP is interesting,[36,37] but it would seem that the coordination sphere of the metal catalyst should have an impact on the rate in virtually any mechanism.

Overall, if one accepts the postulate that an ATRP mechanism involving radical−metal complexes can indistinguishably resemble a free-radical process in a variety of ways, such as monomer reactivity ratios[21−23] or the isotope effects here, then such a mechanism becomes virtually impossible to disprove. At this time, however, the evidence discretely favoring the importance of radical−metal complexes seems very faint.

The observation of indistinguishable KIEs in methyl methacrylate for free-radical polymerization (this work) vs ATRP catalyzed by CuBr/2,2′-bipyridine (this work) vs ATRP catalyzed by CuBr/*N*-propyl-2-pyridinylmethanimine[38] strongly supports identical chain-propagation steps. Strictly, it is important to bear in mind that our results only apply to the chain-propagation step for the mechanism and to the particular systems studied. The diversity of alternative systems for ATRP should be studied, as it is possible that polymerization of other monomers and/or using different catalysts may be accompanied by some contribution of other mechanisms and that other aspects of the mechanism can differ and have important effects. Coordination of radicals to metal centers may have an impact in some reactions without affecting the mechanism of the chain propagation.[61] It was earlier reported that some radicals may be oxidized

to cations or reduced to anions.[62] This may sometimes lead to different products in ATRA.[63] Also, diffusion phenomena or monomer complexation may alter reactivity ratios,[64] and the intermittent activation may lead to a preferential incorporation of one diastereomer.[24]

Conclusions

The predicted and experimental isotope effects for free-radical polymerization correspond very closely. The underprediction of the Cβ KIE based on DFT-calculated transition structures may be taken as suggestion that the structures are early compared to the actual transition state, and this idea is supported by later transition structures found in high-level ab initio calculations for the addition of methyl radical to ethylene. However, the geometric error is likely small, arguably negligible. The KIEs provide an experimental basis for confidence in the accuracy of **10** as a depiction of the physical transition state.

The observed KIEs for free-radical polymerization initiated by AIBN and ATRP initiated by 1:2:1 CuBr:2,2′-bipyridine:ethyl 2-bromoisobutyrate are statistically indistinguishable. Such an observation can never rule out the operation of an alternative mechanism for ATRP that coincidentally exhibits the same KIEs. Our results are also limited to the conditions studied, and the diverse possible conditions for ATRP could in principle proceed by different mechanisms. However, our observations would certainly be considered as supporting identical chain-extending steps in the free-radical and ATRP mechanisms. At the same time, both our experimental results and theoretical predictions call into question the HRH Cα KIE for free-radical polymerization. This compromises the most significant literature observation arguing for a more complicated mechanism for ATRP. For now, the weight of evidence strongly favors a free-radical process for chain extension. For the analogous transition-metal-catalyzed ATRA reactions, the evidence for the importance of metal−radical complexes, when evaluated critically, does not appear to be compelling. In the absence of observable, kinetically viable metal−radical complexes in these reactions, it would appear likely that in general both ATRP and ATRA reactions proceed by identical conventional mechanisms.

Experimental Section

Materials. Methyl methacrylate (ACROS, 99%, inhibited with monomethyl ether hydroquinone) was passed through activated basic alumina to remove the inhibitor. CuBr (Aldrich, 98%) was purified according to the method described by Keller and Wycoff.[65] Methyl methacrylate and 1,2-dichlorobenzene were deoxygenated by sparging with N_2 for 60 min before using.

Free-Radical Polymerizations. Example Procedure. A mixture of 50 mL (46.8 g, 0.47 mol) of methyl methacrylate, 50 mL of 1,2-dichlorobenzene, and 0.23 g (1.40 mmol) of AIBN in a dried Schlenk flask was subjected to three freeze−pump−thaw cycles and then heated to 80 °C. Aliquots were removed periodically and analyzed by GC (CEC-Wax, 30 m × 0.53 mm × 1.0 μm, Chrom Expert Co.) using the dichlorobenzene as internal standard until a conversion of ≈80% was reached. The reaction vessel was then cooled in liquid nitrogen and opened to air, and 0.403 g (2.34 mmol) of hydroxy-TEMPO in 3 mL of 1,2-dichlorobenzene was mixed into the polymer to quench the reaction. The unreacted methyl methacrylate was then reisolated by an initial rapid vacuum distillation followed by a fractional distillation in the presence of hydroquinone.

ATRP. Example Procedure. A dried Schlenk flask containing 0.335 g (2.34 mmol) of CuBr was subjected to three vacuum−nitrogen cycles, and 50 mL (46.8 g, 0.47 mol) of methyl methacrylate, 50 mL of 1,2-dichlorobenzene, and 0.73 g (4.64 mmol) of 2,2′-bipyridine were added. After three freeze−pump−thaw cycles, 0.35 mL (0.465 g, 2.38 mmol) of ethyl 2-bromoisobutyrate was added under N_2 using a degassed syringe, and the stirred reaction mixture was heated to 80 °C. Aliquots were removed periodically and analyzed as described above until a conversion of ≈80% was reached. The reaction was then quenched and the unreacted methyl methacrylate reisolated as described in the previous procedure.

NMR Measurements. Samples were prepared either neat or by diluting 472 mg of methyl methacrylate with $CDCl_3$ to a constant height of 5.0 cm in 5 mm NMR tubes. The ^{13}C spectra were recorded at either 100.5 MHz (four samples, 7.000 s acquisition time, collecting 350 000 points, 190 s delays between pulses) or 125.70 MHz (four samples, 6.001 s acquisition time, collecting 300 032 points, 167 s delays between pulses) using inverse gated decoupling and calibrated $\pi/2$ pulses. Integrations were determined numerically using a constant integration region for each peak. A zeroth-order baseline correction was generally applied, but in no case was a first-order (tilt) correction applied. Six spectra were obtained for each sample of recovered methyl methacrylate along with corresponding samples of methyl methacrylate, prepared identically, that were not subjected to the reaction conditions. The resulting ^{13}C integrations for these spectra are given in the Supporting Information. From the ^{13}C integrations, the KIEs and uncertainties were calculated as previously described.[39]

The samples of methyl methacrylate obtained from both free-radical polymerization and ATRP were contaminated with 2%−9% of 1,2-dichlorobenzene. In a test of the effect of the 1,2-dichlorobenzene on the ^{13}C NMR integrations, a sample spiked with 10% 1,2-dichlorobenzene was analyzed and found to exhibit indistinguishable integrations from a pure sample of methyl methacrylate.

Acknowledgment. We thank NIH Grant GM-45617, NSF (CHE-00-96601 and CHE-00-77917), and The Robert A. Welch Foundation for support of this research.

Supporting Information Available: Energies and full geometries of all calculated structures and NMR integration results for all reactions. This material is available free of charge via the Internet at http://pubs.acs.org.

References and Notes

(1) Matyjaszewski, K., Davis, T. P., Eds. *Handbook of Radical Polymerization*; Wiley-Interscience: Hoboken, 2002.
(2) Matyjaszewski, K., Ed. *Controlled Radical Polymerization*; American Chemical Society: Washington, DC, 1998; Vol. 685.
(3) Matyjaszewski, K., Ed. *Controlled-Living Radical Polymerization: Progress in ATRP, NMP, and RAFT*; American Chemical Society: Washington, DC, 2000; Vol. 768.
(4) Wang, J. S.; Matyjaszewski, K. *J. Am. Chem. Soc.* **1995**, *117*, 5614−5615.
(5) Matyjaszewski, K.; Xia, J. *Chem. Rev.* **2001**, *101*, 2921−2990.
(6) Kamigaito, M.; Ando, T.; Sawamoto, M. *Chem. Rev.* **2001**, *101*, 3689−3745.
(7) Coessens, V.; Pintauer, T.; Matyjaszewski, K. *Prog. Polym. Sci.* **2001**, *26*, 337−377.
(8) Patten, T. E.; Matyjaszewski, K. *Adv. Mater.* **1998**, *10*, 901−915.
(9) Patten, T. E.; Matyjaszewski, K. *Acc. Chem. Res.* **1999**, *32*, 895−903.
(10) Curran, D. P. In *Comprehensive Organic Synthesis*; Trost, B. M., Fleming, I., Eds.; Pergamon: New York, 1992; Vol. 4.
(11) Minisci, F. *Acc. Chem. Res.* **1975**, *8*, 165−171.
(12) (a) Matsumoto, H.; Nikaido, T.; Nagai, Y. *Tetrahedron Lett.* **1975**, 899−902. (b) Matsumoto, H.; Nakano, T.; Takasu, K.; Nagai, Y. *J. Org. Chem.* **1978**, *43*, 1734−1736.
(13) Elzinga, J.; Hogeveen, H. *J. Org. Chem.* **1980**, *45*, 3957−3969.

(14) Tsuji, J.; Sato, K.; Nagashima, H. *Tetrahedron* **1985**, *41*, 5003−5006.
(15) Bland, W. J.; Davis, R.; Durrant, J. L. A. *J. Organomet. Chem.* **1985**, *280*, 397−406.
(16) (a) Bellus, D. *Pure Appl. Chem.* **1985**, *57*, 1827−1838. (b) Martin, P.; Steiner, E.; Streith, J.; Winkler, T.; Bellus, D. *Tetrahedron* **1985**, *41*, 4057−4078.
(17) Kameyama, M.; Kamigata, N.; Kobayashi, M. *J. Org. Chem.* **1987**, *52*, 3312−3316.
(18) van de Kuil, L. A.; Grove, D. M.; Gossage, R. A.; Zwikker, J. W.; Jenneskens, L. W.; Drenth, W.; van Koten, G. *Organometallics* **1997**, *16*, 4985−4994.
(19) Grigg, R.; Devlin, J.; Ramasubbu, A.; Scott, R. M.; Stevenson, P. *J. Chem. Soc., Perkin Trans. 1* **1987**, 1515−1520.
(20) Davis, R.; Groves, I. F. *J. Chem. Soc., Dalton Trans.* **1982**, 2281−2287.
(21) Haddleton, D. M.; Crossman, M. C.; Hunt, K. H.; Topping, C.; Waterson, C.; Suddaby, K. G. *Macromolecules* **1997**, *30*, 3992−3998.
(22) Matyjaszewski, K.; Ziegler, M. J.; Arehart, S. V.; Greszta, D.; Pakula, T. *J. Phys. Org. Chem.* **2000**, *13*, 775−786.
(23) Madruga, E. L. *Prog. Polym. Sci.* **2002**, *27*, 1879−1924.
(24) Matyjaszewski, K. *Macromolecules* **2002**, *35*, 6773−6781.
(25) Wang, J.-S.; Matyjaszewski, K. *Macromolecules* **1995**, *28*, 7901−7910.
(26) Coca, S.; Jasieczek, C. B.; Beers, K. L.; Matyjaszewski, K. *J. Polym. Sci., Part A: Polym. Chem.* **1998**, *36*, 1417−1424.
(27) Qiu, J.; Charleux, B.; Matyjaszewski, K. *Prog. Polym. Sci.* **2001**, *26*, 2083−2134.
(28) Wang, J.-S.; Matyjaszewski, K. *Macromolecules* **1995**, *28*, 7572−7573.
(29) Xia, J.; Matyjaszewski, K. *Macromolecules* **1997**, *30*, 7692−7696.
(30) Matyjaszewski, K.; Paik, H.-j.; Shipp, D. A.; Isobe, Y.; Okamoto, Y. *Macromolecules* **2001**, *34*, 3127−3129.
(31) Kajiwara, A.; Matyjaszewski, K.; Kamachi, M. *Macromolecules* **1998**, *31*, 5695−5701.
(32) Fischer, H. *J. Polym. Sci., Part A: Polym. Chem.* **1999**, *37*, 1885−1901.
(33) Yu, Q.; Zeng, F.; Zhu, S. *Macromolecules* **2001**, *34*, 1612−1618.
(34) Pintauer, T.; Zhou, P.; Matyjaszewski, K. *J. Am. Chem. Soc.* **2002**, *124*, 8196−8197.
(35) Haddleton, D. M.; Clark, A. J.; Crossman, M. C.; Duncalf, D. J.; Heming, A. M.; Morsley, S. R.; Shooter, A. J. *Chem. Commun.* **1997**, 1173−1174.
(36) Haddleton, D. M.; Perrier, S.; Bon, S. A. F. *Macromolecules* **2000**, *33*, 8246−8251.
(37) Wang, X.-S.; Armes, S. P. *Macromolecules* **2000**, *33*, 6640−6647.
(38) Harrisson, S.; Rourke, J. P.; Haddleton, D. M. *Chem. Commun.* **2002**, 1470−1471.
(39) Singleton, D. A.; Thomas, A. A. *J. Am. Chem. Soc.* **1995**, *117*, 9357−9358.
(40) Wong, M. W.; Radom, L. *J. Phys. Chem.* **1995**, *99*, 8582−8588.
(41) (a) Beno, B. R.; Houk, K. N.; Singleton, D. A. *J. Am. Chem. Soc.* **1996**, *118*, 9984−9985. (b) Meyer, M. P.; DelMonte, A. J.; Singleton, D. A. *J. Am. Chem. Soc.* **1999**, *121*, 10865−10874.
(42) Arnaud, R.; Bugaud, N.; Vetere, V.; Barone, V. *J. Am. Chem. Soc.* **1998**, *120*, 5733−5740.
(43) Fischer, H.; Radom, L. *Angew. Chem., Int. Ed.* **2001**, *40*, 1340−1371.
(44) For the addition of formylmethyl radical to acrolein, the transition-state conformer studied was the one that most closely matched the best transition-state conformer for the addition of methyl isobutyryl radical to methyl methacrylate. No effort was made to explore other conformers.
(45) Chuang, Y.-Y.; Coitino, E. L.; Truhlar, D. G. *J. Phys. Chem. A* **2000**, *104*, 446−450. The barrier predicted in UCCSD(T)/cc-pVDZ calculations for reaction R2 in this paper is high, but as exemplified in the discussion, larger basis sets lead to highly accurate barriers.
(46) Kerr, J. A. In *Free Radicals*; Kochi, J., Ed.; Wiley: New York, 1972; Vol. 1, pp 1−36.
(47) (a) Blais, N. C.; Truhlar, D. G.; Garrett, B. C. *J. Chem. Phys.* **1982**, *76*, 2768−2770. (b) Garrett, B. C.; Truhlar, D. G.; Bowman, J. M.; Wagner, A. F.; Robie, D.; Arepalli, S.; Presser, N.; Gordon, R. J. *J. Am. Chem. Soc.* **1986**, *108*, 3515−3516. (c) Allison, T. C.; Lynch, G. C.; Truhlar, D. G.; Gordon, M. S. *J. Phys. Chem.* **1996**, *100*, 13575−13587.
(48) This is based on an experimental rate constant of 3700 M^{-1} s^{-1} and an assumed log *A* of 7.5 ± 0.8. See: Zytowski, T.; Knühl, B.; Fischer, H. *Helv. Chim. Acta* **2000**, *83*, 658−675.
(49) The calculations used the program QUIVER (Saunders, M.; Laidig, K. E.; Wolfsberg, M. *J. Am. Chem. Soc.* **1989**, *111*, 8989−8994). Becke3LYP/6-31G* and MPW1K/6-31+G** frequencies were scaled by 0.9614 and 0.9515, respectively (Scott, A. P.; Radom, L. *J. Phys. Chem.* **1996**, *100*, 16502−16513. Lynch, B. J.; Truhlar, D. G. *J. Phys. Chem. A* **2001**, *105*, 2936−2941). CCSD(T)/6-311+G**, CCSD(T)/6-31G*, QCISD/6-31G*, and Becke3LYP/6-311+G** scalings of 0.97, 0.96, 0.956, and 0.97 were chosen to approximately fit ethylene vibrational frequencies with the scaled Becke3LYP/6-31G* frequencies. It should be noted that the exact choice of scaling factor has little effect—changing the scaling from 0.92 to 1.00 made only 0.001 difference in the prediction of the Cβ KIEs and no change at all in the others.
(50) (a) Bigeleisen, J.; Mayer, M. G. *J. Chem. Phys.* **1947**, *15*, 261−267. (b) Wolfsberg, M. *Acc. Chem. Res.* **1972**, *5*, 225−233. (c) Bigeleisen, J. *J. Chem. Phys.* **1949**, *17*, 675−678.
(51) Bell, R. P. *The Tunnel Effect in Chemistry*; Chapman & Hall: London, 1980; pp 60−63.
(52) (a) Singleton, D. A.; Hang, C.; Szymanski, M. J.; Meyer, M. P.; Leach, A. G.; Kuwata, K. T.; Chen, J. S.; Greer, A.; Foote, C. S.; Houk, K. N. *J. Am. Chem. Soc.* **2003**, *125*, 1319−1328. (b) Singleton, D. A.; Schulmeier, B. E.; Hang, C.; Thomas, A. A.; Leung, S.-W.; Merrigan, S. R. *Tetrahedron* **2001**, *57*, 5149−5160. (c) Singleton, D. A.; Hang, C. *J. Org. Chem.* **2000**, *65*, 7554−7560. (d) Singleton, D. A.; Hang, C. *J. Am. Chem. Soc.* **1999**, *121*, 11885−11893.
(53) From the Supporting Information in ref 38, the KIEs were apparently determined by comparing spectra for pure standard starting material versus substantially impure recovered material. Also, the integration ranges employed for the standard do not appear to match those for recovered material. This procedure appears to have worked satisfactorily for most of the KIEs in ref 38, but our experience with the effect of impurities and variable integration ranges would suggest caution.
(54) Fischer, H. *J. Am. Chem. Soc.* **1986**, *108*, 3925−3927.
(55) Matyjaszewski, K. *Chem.—Eur. J.* **1999**, *5*, 3095−3102.
(56) Bland, W. J.; Davis, R.; Durrant, J. L. A. *J. Organomet. Chem.* **1984**, *260*, C75−C77.
(57) Davis, R.; Furze, J. D.; Cole-Hamilton, D. J.; Pogorzelec, P. *J. Organomet. Chem.* **1992**, *440*, 191−196.
(58) For the simulation, the initial concentrations of R−X, M^{+n}, and alkene were 1, 0.001, and 1 M, respectively. The coupling of R$^\bullet$ was assumed to occur at 10^9 M^{-1} $s^{-1.}$ The apparent order of the alkene from initial rates would depend on how far into the reaction the rate was measured.
(59) (a) Bagdasar'ian, K. S.; Sinitsina, Z. A. *J. Polym. Sci.* ***1961***, *52*, 31−38. (b) Barton, S. C.; Bird, R. A.; Russell, K. E. *Can. J. Chem.* **1963**, *41*, 2737−2742.
(60) (a) Dolgoplosk, B. A.; Parfenova, G. A. *Z. Obshch. Khim.* **1957**, *27*, 3083−3087. (b) Denisov, E. T.; Khudyakov, I. V. *Chem. Rev.* **1987**, *87*, 1313−1357.
(61) (a) Woodworth, B. E.; Metzner, Z.; Matyjaszewski, K. *Macromolecules* **1998**, *31*, 7999−8004. (b) Pintauer, T.; Tsarevsky, N. V.; Kickelbick, G.; Matyjaszewski, K. *Polym. Prepr.* **2002**, *43*, 221−222.
(62) Matyjaszewski, K. *Macromolecules* **1998**, *31*, 4710−4717.
(63) Udding, J. H.; Tuijp, K. J. M.; vanZanden, M. N. A.; Hiemstra, H.; Meyerstein, D. *J. Org. Chem.* **1994**, *59*, 1993−2083.
(64) (a) Roos, S. G.; Mueller, A. H. E.; Matyjaszewski, K. *Macromolecules* **1999**, *32*, 8331−8335. (b) Shinoda, H.; Matyjaszewski, K. *Macromolecules* **2001**, *34*, 6243−6248. (c) Shinoda, H.; Miller, P. J.; Matyjaszewski, K. *Macromolecules* **2001**, *34*, 3186−3194. (d) Lutz, J.-F.; Kirci, B.; Matyjaszewski, K. *Macromolecules* **2003**, *36*, 3136−3145.
(65) Keller, R. N.; Wycoff, H. D. *Inorg. Synth.* **1946**, *2*, 1−4.

MA035310R